ISSN : 2800-1729 **Edition : Vol 4. Num 2 (2025)**

Biopolymer Applications Journal

Editor in chief:
Pr. HAMMICHE Dalila

UNIVERSITÉ ABDERRAHMANE MIRA - BEJAIA
FACULTÉ DE TECHNOLOGIE

www.univ-bejaia/baj

ISSN : 2800-1729

Table of content

Biopolymer Applications Journal
e-ISSN: 2800-1729
Samira SAHI et al. Vol 04. N°2, 2025, pp.01.-04

Study of the physical and mechanical properties of a naturally reinforced composite after several recycling processes

Samira SAHI[1*]; Naima TOUATI[1]; Lamia BENAZZOUZ[2]; Ahlam BEN BELLIL[2]
1 Laboratory of Advanced Polymer Materials. Department of Technical Sciences. Faculty of technology. University A. Mira of Bejaia. Bejaia (06000). Algeria.
2 Department of Process Engineering. Faculty of technology. University A. Mira of Bejaia. Bejaia (06000). Algeria.
**Corresponding author : samira.sahi@univ-bejaia.dz*
Received: 25 March, 2025; Accepted: 18 May, 2025; Published: 4 July, 2025

Abstract
Composites based of Poly (vinyl Chloride) (PVC) reinforced with maize flour (MF) at proportion of 30 (%.Wt) were prepared. The objective of this work is to study the effect of the number cycle of the recycling in the physical, chemical and mechanical properties in this composite. Different characterization techniques were used to study the effect of the number of recycling cycles on the mechanical, physical and chemical properties of the materials developed. The results recorded after three cycles of recycling show an increase in tensile strength, in Young's modulus and in water absorption of composites. However, a decrease in hardness is recorded. FTIR analysis showed no change in the absorption bands after recycling.
Keywords: *Composites, recycling, PVC, vegetable filler.*

I. Introduction

The accumulation of plastic waste in the environment has led to overcrowding of landfill sites and pollution of soil and marine environments. A number of solutions have been put in place to reduce their impact on the environment. Like giving these polymers a new lease of life through recycling. So, in the interests of the environment, we need to improve recycling processes and encourage the use of materials derived from abundant, recyclable and renewable natural resources. To this end, numerous environmental standards (ISO 14 001) [1] have been created to contribute to sustainable development goals. These standards have had a major impact on the industry, particularly in the development of new composite materials based on natural fibers. Natural fibers are a new trend in reinforcements and supplements, used to replace synthetic materials and related products. The development of natural fibre-reinforced composites has been one of the notable achievements in materials science over the last century [2-5]. In recent years, composite materials have come to occupy a prominent place in various fields. However, the development of these materials must be accompanied by the introduction of industrial solutions capable of processing production waste and end-of-life products in compliance with the regulatory framework [6].

Polymer matrix composites are used on a large scale in a variety of industrial applications (transport, construction, etc.). However, their recyclability, perceived as difficult or at least perfectible due to their heterogeneity, can be an obstacle to their wider penetration of certain markets. Some users may prefer alternative materials that are easier to recycle to composites. Environmental concerns and regulatory pressure have prompted manufacturers in the composites sector to develop recycling and recovery solutions, whether in terms of materials, heat/energy or chemicals. Against this regulatory backdrop, various industry initiatives are aiming to set up dismantling/recycling/recovery channels for these materials, either by application sector or across the board [7].

The aim of this research is to study the possibility to prepare PVC/maize flour composite and the study of the effect of the number cycle of the recycling in the physical, chemical and mechanical properties in this composite.

II. Material and methods

II.1 Materials

The PVC used is the SE1200 type and has been utilized as a matrix for the development of the different samples. Glycerol was procured from Chemopharma BIOCHEM. The maize flour with a diameter ≤ 300 µm was obtained from an Algerian cereals company, Algeria. The proportion between the maize flour and the glycerol was 70/30 (wt/wt). This percentage is used to obtain flexible materials.

Additives were added for the preparation of the various formulations, including dioctyl phthalate (DOP) as a plasticizer, a Ca/Zn-based thermal stabilizer and stearic acid as a lubricant.

II.2 Methods

Samples preparation

PVC (F0) and PVC/MF composite at ratio of 70:30 (F30) was prepared by two processing methods, namely: calendaring and compression molding. The blend was introduced into a T6HK8 type mixer for 15 min at the rate of

2000 rpm and at the working temperature of 80°C. Before unloading, this mixture cooled at 40°C. Then the blend introduced into a two-roll mixer at a temperature of 140°C. The prepared mixture is introduced into the platens of the brand table press at 170°C with a pressure of 300 kN during 5 minutes. Pieces of hard plastic of 250×250×2 mm^3 are obtained and cooled to room temperature, which will be used for cutting samples in the form of dumbbells.

Recycling process

The PVC and PVC/FM composite are recycled using a brabender. The recycling stage was carried out using a 'Brabender Gmbh & Co KG' internal mixer. The previously prepared plates, which had been cut into small fragments, were poured into the Brabender chamber (hopper) at a temperature of 180°C, a speed of 50 rpm and a residence time of 5 minutes in order to obtain a paste. The Brabender is controlled by a computer running WIN MIX software.

Tensile properties

Measurements of the tensile properties were performed using a Shimadzu tensile testing machine (Model Autograph AGS-X 10kN). Measurements were performed at a 10 mm min^{-1} crosshead speed at ambient temperature. five specimens were tested. The Young's modulus. strain and stress were determined.

Hardness

This technique consists of the application of a force designed to force the pointed steel needle (punch) of the Shore-D durometer onto a 1x6 cm^2 plate in accordance with standard NF T51-109.

Spectroscopy analysis (FTIR)

FTIR spectra were recorded using an infrared spectrophotometer Fourier Transform Model SHIMADZU FTIR using film samples. The spectra were recorded in a transmittance mode from 4000 to 400 cm^{-1} at a resolution of 4 cm^{-1}.

Water absorbance test

The water uptake is determined in standard ASTM-7031-04. The measurement consists of submerging the specimen into distilled water at room temperature with agitation. The samples are then weighed at intervals of 24 hours until the weight have stabilized. The rate of water uptake is measured using the following equation:

$$\Delta m(\%) = \frac{m - m_0}{m_0} \times 100 \qquad (1)$$

With:

m_0: Sample weight before immersing.

m: Sample weight after immersing.

III. Results and discussion

Tensile properties

Figure 1 shows the change in stress at break of PVC/MF composites as a function of the number of recycling cycles. It can be seen that recycling has not affected this property for virgin PVC, but an increase in stress is recorded for composite after the first recycling cycle compared with before recycling. This may be due to the reinforcement of the matrix by the filler after recycling and the increase in bond strength between the filler and the matrix [8]. After the second and third recycling cycles, we did not record any significant change in this parameter, which means that recycling does not affect this property.

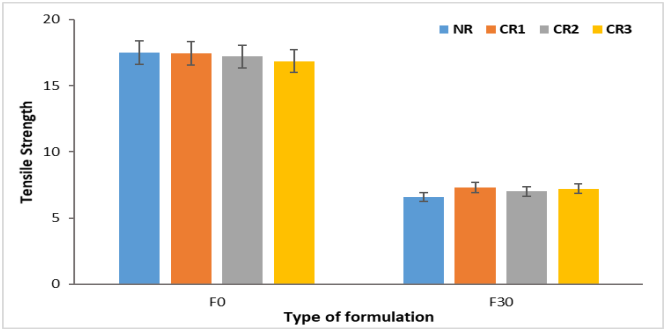

Figure 1. Tensile Strength of pure PVC and PVC/MF composite, before and after recycling.

The variation in Young's modulus of PVC and composites at 30% load is shown in Figure 2. The results show that the Young's modulus increases with the incorporation of the MF into the PVC matrix. This behavior is attributed to the rigid phase of the dispersed fillers, which imparts high rigidity to the PVC matrix. This increase could also be explained by the increased crystallinity of the material after addition of the filler. Sahi et al. [9] have indicated that Young's modulus generally increases with increasing cellulose filler content. However, it was found that the Young's modulus of PVC and the PVC/MF composite for a filler content of 30% increased with the number of recycles.

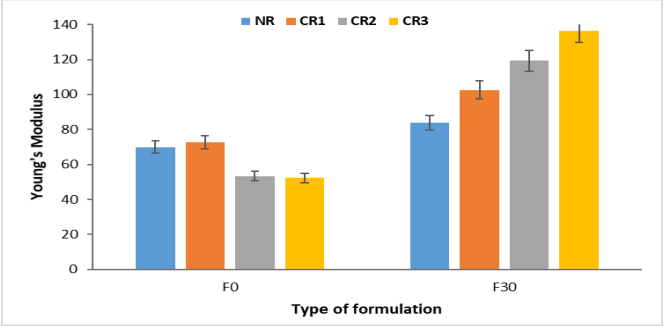

Figure 2. Young's Modulus of pure PVC and PVC/MF composite, before and after recycling.

Hardness

The variation in hardness is shown in Figure 3. It can be seen that hardness increases after the introduction of the filler compared with virgin PVC. This increase can be explained

by the fact that adding an organic filler to a material can strengthen its structure and improve its hardness [10, 11]. For the recycled PVC matrix, the hardness increased after the first cycle, then a decrease was recorded from the second cycle onwards. On the other hand, for the various composites, the hardness decreased continuously with the number of cycles. This can be explained by the fact that the recycling process can introduce impurities or defects into the crystalline structure of the material, and recycling can lead to heating cycles that can alter the microstructure of the material, thus influencing its hardness [12].

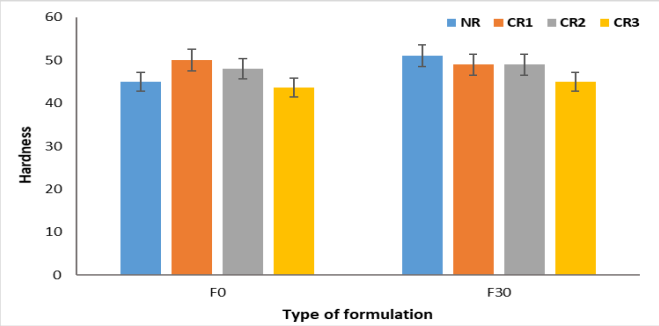

Figure 3. Hardness of pure PVC and PVC/MF composite, before and after recycling.

Water absorbance test

Figure 4 shows the evolution of the water absorption of un-recycled and recycled PVC and PVC/MF composite as a function of immersion time in water. It can be seen that virgin PVC (F0) does not absorb water. This is due to the fact that PVC is a hydrophobic polymer which often records very low water absorption [13]. After recycling, it can be seen that for F30 formulations, an increase in water absorption was recorded from the second recycling cycle. It increased from 11.07% for the F30 NR formulation to 11.27%, 15.87% and 20.80% for the F30 1RC, F30 2RC and F30 3RC formulations respectively. These results can be attributed to the structural changes produced by recycling, which can make PVC/FM composites more permeable to water.

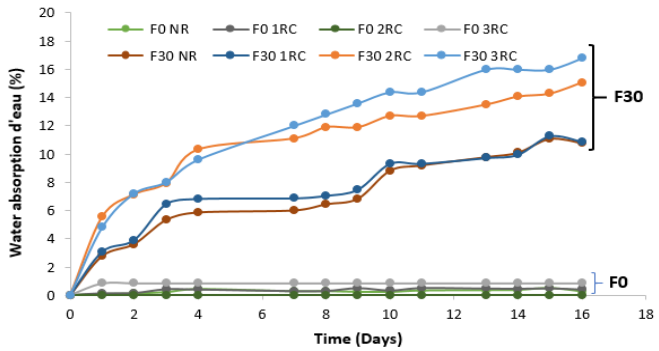

Figure 4. Water absorption of PVC and PVC/MF composites, before and after recycling.

FTIR analysis

The FTIR spectra of corn is shown in Fig. 5. The spectra of maize flour have characteristic profiles to native starch. According to the literature [9, 14]. the chemical functions for each absorption band which appears on the FTIR spectra of starch are given as follow:

There are three characteristic bands of starch between 990 cm^{-1} and 1160 cm^{-1}. attributed to C-O bond stretching. The bands at around 1150 cm^{-1}. 1080 cm^{-1} were characteristic of C-O-H in starch. and the band between 990 cm^{-1} and 1030 cm^{-1} was characteristic of the anhydroglucose ring O-C stretch. The band at 1655 cm^{-1} is attributed to the water adsorbed in the amorphous region of starches. The band at 2920 cm^{-1} is characteristic of C-H stretch. An extremely broad band due to hydrogen-bonded hydroxyl groups appeared at 3400 cm^{-1} which ascribed to the complex vibrational stretches coupled with free. inter and intramolecular bound hydroxyl groups. which made up the gross structure of starch.

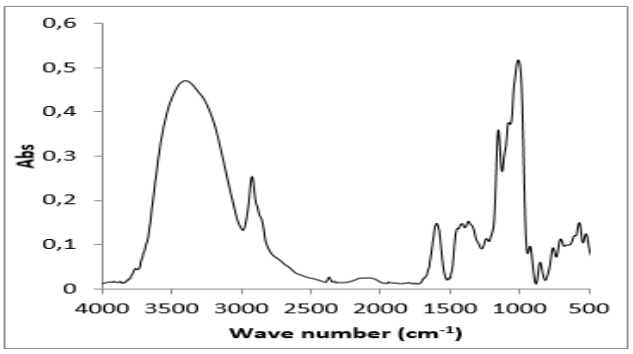

Figure 5. FTIR spectra of MF.

The FTIR spectra of recycled (1R, 2R and 3R) and non-recycled of PVC and PVC/MF composites with a 30% filler content are shown in Figures 6 and 7 respectively. It can be seen from all the spectra that recycling causes neither the disappearance nor the formation of new absorption bands. However, there was an increase in the intensity of certain bands during recycling, namely those centered at 1720 cm^{-1} relating to carbonyls groups.

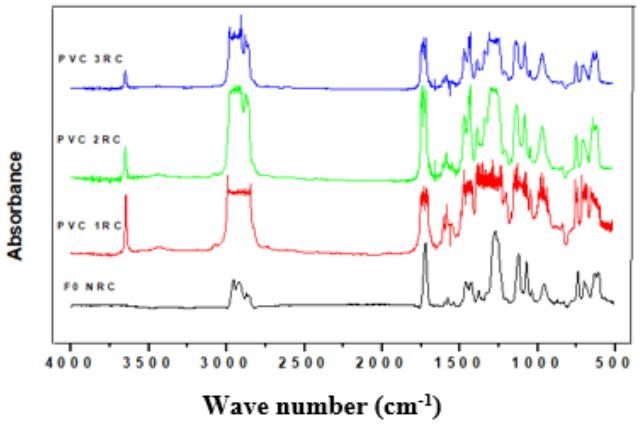

Figure 6. FTIR spectra of PVC before and after recycling.

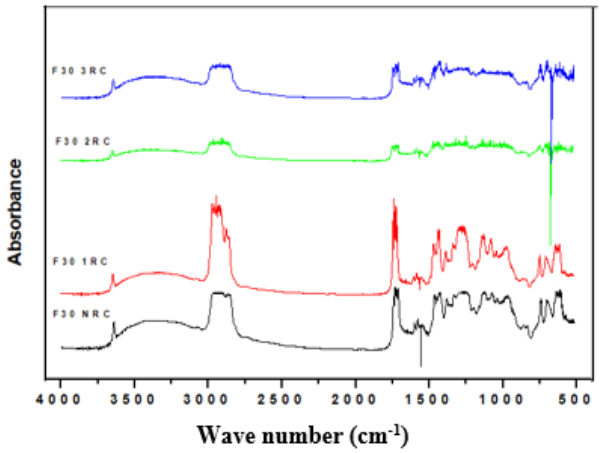

Figure 7. FTIR spectra of PVC/MF before and after recycling.

IV. Conclusions

Study consists on the incorporation of maize flour in PVC matrix and to study the feasibility of its recycling.

Analysis of the experimental results recorded before and after three recycling cycles has enabled us to draw the following main conclusions:

- The stress at break of PVC and PVC/FM composites was not affected by recycling.
- The Young's modulus of PVC decreased after the second and third recycling cycles. However, a continuous increase in stiffness was observed after each recycling cycle at a loading rate of 30%.
- PVC hardness showed an increase after the first recycling cycle, followed by a slight decrease after the second and third recycling cycles. For the filled material, an increase in hardness was observed after each cycle.
- The water absorption test revealed that the water absorption of PVC showed a negligible increase after the three recycling cycles and that an increase in this parameter was recorded after the third and second recycling for the material filled with 30% MF.
- Analysis of the FTIR spectra enabled us to determine the main changes induced by the three recycling cycles for PVC and the PVC/MF composite.

Conflict of interest

The authors declare that they have no conflict for financial interests or personal relationships that how can influence the work reported in this paper.

References

[1] D. Triebert, H. Hanel, M. Bundt, K. Wohnig, Solvent-based recycling. In Circular Economy of Polymers: Topics in Recycling Technologies. ACS Symposium Series 1391. 33-59. 2021.

[2] L. Avérous. Biodegradable multiphase systems based on plasticized starch. Journal of macromolecular Science. Part C: Polymer Review 44. 231-274. 2004.

[3] M. Kim. Evaluation of degradability of hydroxypropylated potato starch/polyethylene blend films. Carbohydrate Polymer 54. 173-181. 2003.

[4] D. Ray. B. K. Sarkar. N. R. Rose. Impact fatigue behavior of vinylester matrix composites reinforced with alkali treated jute fibres. Composites: Part A 33. 233-241. 2001.

[5] Y. Cao. S. Shibata. I. Fukumoto. Mechanical properties of biodegradable composites reinforced with bagasse fibre before and after alkali treatments. Composites : Part A 37. 423-429. 2006.

[6] W. Sikorska, M. Musioł, Zawidlak- B. Węgrzyńska, J. Rydz. End-of-Life Options for (Bio)degradable Polymers in the Circular Economy. Advances in Polymer Technology 6695140, 18 pages. 2021.

[7] P. Krawczak. Recyclage des matériaux composites : Etat de l'art et perspectives. Journée Technique "Le recyclage et la valorisation des matériaux composites", May 2015, Méaulte, France.

[8] R. Scaffaro, A. Di Bartolo, N. Tz Dintcheva. Matrix and Filler Recycling of Carbon and Glass Fiber-Reinforced Polymer Composites: A Review. Polymers 13. 3817. 2021.

[9] S. Sahi, H. Djidjelli. Utilisation de l'amidon comme charge biodégradable dans les matériaux composites polyéthylène basse densité/amidon. Annale de Chimie et Science des matériaux 38 189-202. 2013.

[10] M. B. Uctasli, H. D. Arisu, L. V. Lasilla, P. K. Valittu. Effect of preheating on the mechanical properties of resin composites. European Journal of Dental 2 263-268. 2008.

[11] D. Tantbirojn, S. Chongvisal, D. G. Augustson, Versluis. A Hardness and postgel shrinkage of preheated composites. Quintessence International 42. 51-9. 2011.

[12] I. Ben Amor, O. Klinkova, M. Baklouti, R. Elleuch, I. Tawfiq. Mechanical Recycling and Its Effects on the Physical and Mechanical Properties of Polyamides. Polymers (Basel) 15. 4561. 2023.

[13] A. Asadinezhad, M. Lehocký, P. Sáha, M. Mozetič. Recent Progress in Surface Modification of Polyvinyl Chloride. Materials (Basel). 5. 2937-59. 2012.

[14] S. Sahi, H. Djidjelli, A. Boukerrou. Biodegradation study of bio-corn flour filled low density polyethylene composites assessed by natural soil. Journal of Polymer Engineering 36. 245-252. 2016.

Biopolymer Applications Journal ***Nadira BELLILI et al. Vol 4, N°2, 2025, pp. 05-09***
e-ISSN : 2800-1729

Effect of physical treatment on the performance of thermoplastic matrix composites with natural fillers

Nadira BELLILI[1, 2*]; Badrina DAIRI[1, 2]; Nadjia RABEHI[1]
[1]*Department of Process Engineering, University of 20Aout – 1955, Skikda, Algeria.*
[2]*Department of Process Engineering, Faculty of Technology, Laboratory of Advanced Polymer Materials (LMPA), A. Mira University , Bejaia, Algeria.*
Corresponding author: n.bellili@univ-skikda.dz*
Received: 27 March, 2025; Accepted: 28 May, 2025; Published: 4 July, 2025

Abstract
Date stone flour was, valorized for use as a reinforcement in the manufacture of polyvinyl chloride matrix composites. Gamma irradiation was, used to improve PVC/FND interfacial adhesion. A reduction in the hydrophilic character of the filler after treatment was, demonstrated by the decrease in the water absorption rate of irradiated DSF -reinforced composites, and this was, confirmed by the good dispersion of the treated filler in the matrix, observed by optical microscopy. As a result, better mechanical properties were, obtained.
Keywords: *Date stone flour, Polyvinyl chloride, Gamma irradiation, Polymer matrix composite.*

I. Introduction

Polyvinyl chloride (PVC) is a thermoplastic polymer with good resistance to moisture and fire. Worldwide demand for PVC exceeds 35 million tonnes a year. In terms of tonnage and consumption, it ranks second only to polyethylene in the plastics industry. It is, used to manufacture a wide range of products with different properties at relatively low cost [1, 2].
In recent decades, lignocellulosic natural fiber/polymer composites have attracted the attention of many researchers because of their environmental adaptability and biodegradability [3 - 6].
The valorization of natural wastes such as date pits by using them in the preparation of thermoplastic matrix composite materials provides a highly interesting alternative to environmental problems and the probable depletion of fossil resources. Date pits are generally, removed from dates before consumption, and rather than being discarded, they can be processed into a form of flour and used in a variety of culinary applications, including as an ingredient in pastry recipes due to its richness in dietary fiber, antioxidants and some minerals such as calcium and potassium.
Date pit fiber is attracting increasing attention from researchers. However, the majority of research has focused on the use of these pits in the form of activated carbon, a livestock feed supplement, and in traditional medicine. For their antimicrobial and antiviral properties, they are, used in the preparation of citric acid and proteins.
This material is an inexhaustible biomass available in Algeria, where production is approximately 1,100,000 tons per year. It is, the abundance of this waste that motivated the choice of date kernel flour as a filler in the manufacture of composite materials.
However, the preparation of composite materials based on cellulosic fillers is, hampered by the highly hydrophilic character of the fibers, which is, associated with poor interfacial compatibility with hydrophobic polymer matrices, as well as a loss of mechanical properties after moisture absorption. In this study, the filler used was, modified by physical treatment such as gamma irradiation and the effect of different doses of gamma radiation (10,15 and 20 kGy) on the mechanical, physical and morphological properties of polyvinyl chloride (PVC)/date stone flour (DSF) composites was investigated.

II. Material and methods

Manufactured type 3000H PVC was, used to prepare the formulations. The various additives (plasticizer, thermal stabilizer, lubricant) and the filler used are, mixed until the mixture becomes homogeneous. The natural filler used is date stone flour (DSF). The torrefied and crushed date stones were, brought in from the wilaya of BISKRA. Sheets 0.5 mm thick of F0 and untreated F20 (20% filler) blends, and treated with

Table.1: Physicochemical properties of polyvinyl chloride

Properties	Measurement methods	Units	Values
Viscosity	ASTM D 1243	CSt 1 CSt = 10^{-6} m²/s	0, 89-1,03
Color			White
Density	ASTM D 1885	g/cm^3	0,481-0,561
Particle size <40µm	ASTM D 1921	%	Max.0, 5
Volatility	CIRES 03.05	%	Max.0, 3

γ-radiation at doses of 10, 15 and 20 kGy (noted: F20, F20T10kGy, F20T15kGy and F20T20kGy respectively) were prepared using a calender. The temperature along the two-roll mixer was, maintained at 160°C, for a residence time of 15 min. The sheets were, then cut into the appropriate shape for characterization.

The properties of the PVC/DSF composites produced are then determined by measuring mechanical properties, water absorption rate, and optical microscope analysis.

For tensile tests, the specimens used in accordance with the dumbbell standard have the dimensions reported in Table 2.

Table 2. Dimensions of the test pieces

Total length, min(L3)		Width (b)	Distance between marks (L0)
Specimen (method B)	115	6	25

This test allows the values of elongation and breaking stress to be, recorded and Young's modulus to be, deduced using a JJ-TEST tensile testing machine.

The water absorption of the composites was, analyzed by immersing the samples in distilled water at room temperature, with periodic monitoring of the specimen weight increase every 24 hours.

The water absorption of the composites was calculated using the following equation:

$$Water\ absorption\ rate\ (\%) = \frac{(m_0 - m)}{m_0} \times 100$$

The surface condition of the composites and the dispersion of the DSF in the PVC matrix were visualized using optical microscopy from mark OPTIKA Microscopies ITALY with a magnification of HC4x0.1 160/0.17.

III. Results and discussion

A. Mechanical properties

The effect of loading and gamma irradiation on the mechanical properties of irradiated and non-irradiated composites was, followed by the change in Young's modulus, stress and elongation at break.

The variation in Young's modulus of the various PVC/DSF samples, untreated and treated with gamma irradiation are, shown in Figure 1.

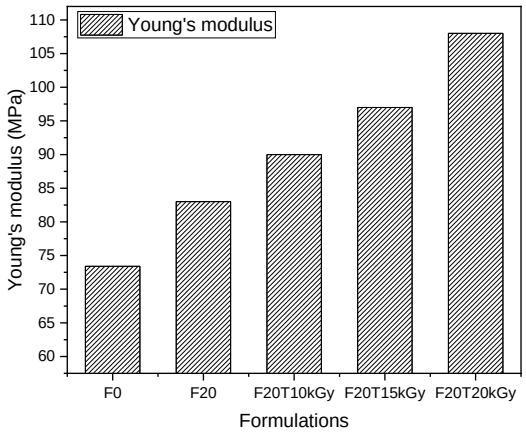

Figure 1. Tensile modulus of PVC matrix and its composites reinforced with unirradiated and irradiated DSF at various doses of gamma radiation

Figure 1, shows that the presence of date stone flour in the PVC matrix increases Young's modulus compared with virgin PVC. The majority of research studies have found an increase in composite stiffness accompanied by an increase in Young's modulus due to the use of a rigid filler [7-9].

Similar results were, reported by DJIDJELI et al. [10] and SAPUANA et al. [11], where they attributed this behavior to the rigid phase of dispersed olive pomace flour, which imparts high stiffness to the polymer matrix. Composites reinforced with the irradiated filler showed high modulus compared with untreated composites. The irradiation process increases the adhesion between DSF particles and PVC matrix by decreasing the hydrophobicity of the DSF particles; this is consistent with the results derived from the water, absorption rate measurements.

Young's modulus increased with increasing irradiation dose. Similar observations have been made by other researchers regarding the effect of gamma irradiation on the elimination of moisture from composites and the improvement of their mechanical properties [12- 14].

The variation in stress and elongation at break before and after incorporation of untreated and treated filler at different irradiation doses are, shown in Figure 2. and Figure 3.

A decrease in stress and elongation at break is, observed for composites filled with untreated DSF compared to those filled with untreated PVC. These results are in agreement with many other works, such as BELLILI et al [7] and DAIRI et al. [9].

This loss, in stress, and strain is due to poor interfacial adhesion between the PVC and date stone flour, and can also, be explained by poor filler dispersion, and consequently the formation of agglomerates, responsible for material fragility. An improvement in stress at break was, observed for treated composites compared to untreated composites.

Chemical changes in cellulose after irradiation are the consequence of unimolecular or bi-molecular radical reactions.

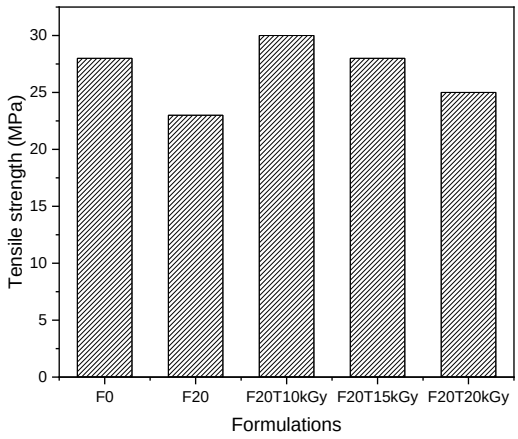

Figure 2. Tensile strength of PVC matrix and its composites reinforced with unirradiated and irradiated DSF at various doses of gamma radiation

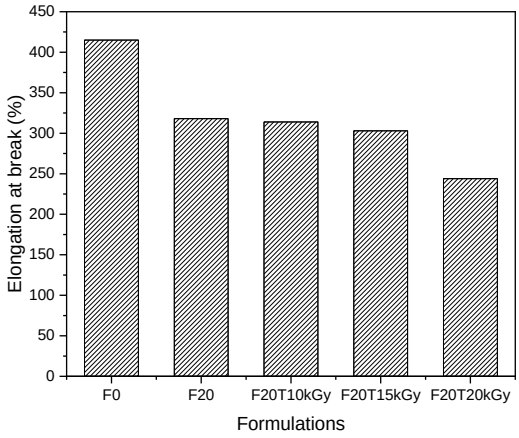

Figure 3. Elongation at break of PVC matrix and its composites reinforced with unirradiated and irradiated DSF at various doses of gamma radiation

Scission can lead to the opening of the anhydroglucose ring or the breaking of glucoside bonds. In both cases, carbonyl groups are, produced as a result, of chain scission into small fragments, there is, the possibility of conformational changes leading to increased intermolecular hydrogen bonding, leading to reinforcement of the three-dimensional structure. They found that at low doses of irradiation, dehydrogenation of cellulose by gamma radiation led to the formation of intermolecular bonds, resulting in increased tensile strength.
Takács E. et al. [15] found that intermolecular hydrogen bonds can replace intramolecular hydrogen bonds more and more as the irradiation dose increases. However, it is possible to produce cross-linking between neighboring chains by means of the radicals produced.

B. Measurement of water absorption rate

The evolution of the water absorption rate of PVC/DSF composites at different irradiation doses and as a function of immersion time is, illustrated in Figure 4.
Figure 4. The evolution of the water absorption rate of PVC/DSF composites at different irradiation doses, as a function of immersion time.

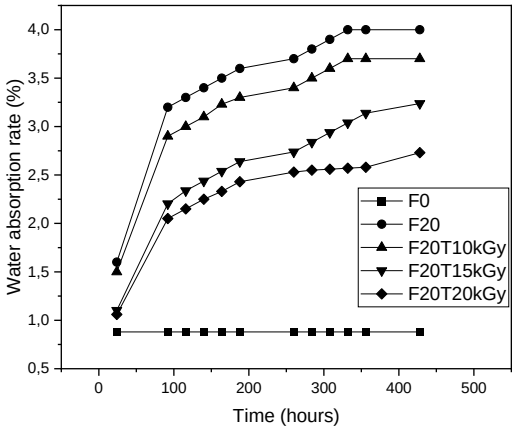

Figure 4. The evolution of the water absorption rate of PVC/DSF composites at different irradiation doses, as a function of immersion time.

The rate of water absorption increases with immersion time and after the addition of 20% DSF to the PVC matrix. This phenomenon is, attributed to the filler's high affinity with water. However, date stone flour is rich in hydroxyl groups, which form hydrogen bonds with water molecules.
Composites reinforced with irradiated filler absorbed less water than untreated composites. The lowest water absorption rates were, recorded by composites treated at 10 and 15 kGy.
The functional groups formed after irradiation react with the OH hydroxyl groups on the flour surface, preventing the cellulose flour from hydrogen bonding with water, thus reducing the amount of water absorbed.
For composites reinforced with the 10, 15 and 20kGy irradiated filler, maximum water absorption rates are, estimated at 3.5, 3.7 and 4% respectively. For virgin PVC, a very low water uptake of around 0.0414% was, recorded in 24 hours, and no more than 0.1904% in 30 days. This is due to the apolar nature of this polymer, which gives it a hydrophobic character, as confirmed by BELLILI et al [7].

C. Optical characterization

The dispersion of treated and untreated date stone flour in the PVC matrix was, verified by optical microscopy, and the micrographs obtained are, shown in Figure 5.
The micrograph of F0 shows a single phase, whereas that of the matrix reinforced with untreated filler shows the appearance of a phase corresponding to the filler, dispersed in another phase corresponding to the matrix. Date stone flour agglomeration was, observed in images of formulations containing untreated filler. This phenomenon was, explained by the poor dispersion of the hydrophilic filler in the hydrophobic matrix. Micrographs of composites reinforced with the irradiated filler showed fewer agglomerates, and the best dispersion was, observed for composites treated at 10 kGy. It can be, concluded that gamma irradiation treatment reduced the hydrophilic character of the filler, resulting in its good dispersion in the PVC matrix. This result confirms the results obtained by measuring the water absorption rate.

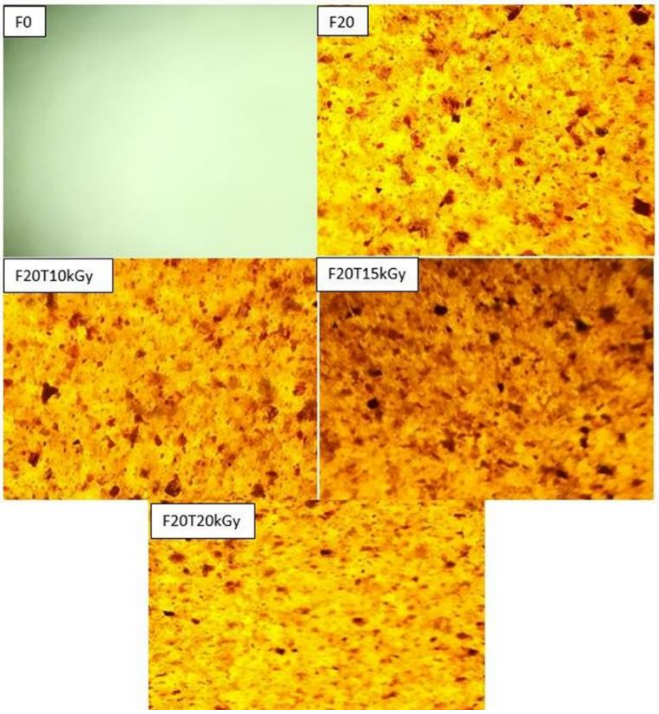

Figure 5. Micrographs of treated and untreated filler-reinforced composites obtained by optical microscopy

IV. Conclusions

In view of the results obtained, the following conclusions can be, drawn:

Mechanical characterization of the composites showed that:

- The behavior of the rigid phase of dispersed date stone flour gives high stiffness to the PVC matrix, leading to an increase in Young's modulus.
- A loss of stress and, strain is, observed due to poor interfacial adhesion between PVC and untreated date stone flour.
- Gamma irradiation-induced scission of chains into small fragments leads to the possibility of conformational changes, leading to an increase in intermolecular hydrogen bonding, which in turn increases tensile strength.

Physical characterization by measuring water absorption rates has enabled us to deduce that:

- The high affinity of the filler with water leads to an increase in the water absorption rate after the addition of 20% DSF to the PVC matrix. The interaction of the functional groups formed after irradiation with the OH hydroxyl groups on the flour surface decreased the amount of water absorbed.
- Micrographs obtained by optical microscopy showed that untreated date stone flour particles tended to aggregate and form agglomerates in the PVC matrix. In contrast, less agglomeration and better dispersion were, observed for composites reinforced with treated filler.

References

[1] M S-Shojai, G R-Bakhshandeh. Recycling of PVC wastes. Polymer Degradation and Stability, 96, 404 – 415, 2011.

[2] N. Yarahmadi, I. Jakubowicz, L. Martinsson. PVC floorings as post-consumer products for mechanical recycling and energy recovery. Polymer Degradation and Stability, 79, 439–448, 2003.

[3] H. Djidjelli, A. Boukerrou, A. Rabouhi, R. Founas, M. Kaci, O. Zefoun, N. Djillali, L. Belmouhoub. Effect of Olive Residue Benzylation on the Thermal and Mechanical Properties of Poly (vinyl chloride)/Olive Residue Composites. Journal of Applied Polymer Science.107, 1459–1465, 2008.

[4] M. N. Belgacem, M. Abdelmouleh, S. Boufi, A. P. Duarte, A. Ben Salah , A. Gandin. Modification of cellulosic fibers with functionalized silanes: Development of surface properties. International Journal of Adhesion and Adhesives, 24, 43–54, 2004.

[5] W. K. El-Zawawy, M. M. Ibrahim, A. Dufresne, A. F. Agblevor. Banana fibers and microfibrils as lignocellulosic reinforcements in polymer composites. Carbohydrate Polymers, 81, (4), 811-819, 2010.

[6] H. Ku, H. Wang, N. Pattarachaiyakoop, M.A. Trada. Review on the tensile properties of natural fiber reinforced polymer composites. Composites: Part B, 42, 856–873, 2011.

[7] N. Bellili, H. Djidjelli, A. Boukerrou, C. Barres, F. Fenouillot. Mechanical and Thermal Properties of Poly (Vinyl chloride) / Olive Residue Flour Blends Treated by Gamma Irradiation. Journal of Vinyl and Additive Technology. 22, (3), 273–278, 2016.

[8] B. Dairi, N. Bellili , N. Hamour, A. Boulassel, H. Djidjelli, A. Boukerrou , R. Bendib. Cork waste valorization as reinforcement in high-density polyethylene matrix. Materials Today: Proceedings, 53, 117–122, 2022.

[9] B. Dairi, H. Djidjelli, A. Boukerrou. Study and Characterization of Composites Materials Based on Poly (Vinyl Chloride) Loaded with Wood Flour. Journal of Materials Science and Engineering A, 3, (2), 110-116, 2013.

[10] H. Djidjelli, D. Benachour, A. Boukerrou, O. Zefouni, J. Martinez- Véga, J. Farenc, M. Kaci. Thermal, dielectric and mechanical study of poly (vinyl chloride)/olive pomace composites. Express Polymer Letters, 1, (12), 846–852, 2007.

[11] S.M. Sapuana, D. Bachtiar. Mechanical Properties of Sugar Palm Fiber Reinforced High Impact Polystyrene Composites. Procedia Chemistry, 4, 101 – 106, 2012.

[12] M. M. EL-Zayat, A. Abdel-Hakim, M. A. Mohamed. Effect of gamma radiation on the physic-o-mechanical properties of recycled HDPE/modified sugarcane

bagasse composite. Journal of Macromolecular Science Part A. Pure and Applied Chemistry, 56, 127–135, 2019.

[13] H. A. Raslan, E. S. Fathy, R. M. Mohamed. Effect of gamma irradiation and fiber surface treatment on the properties of bagasse fiber reinforced waste polypropylene composites. International Journal of Polymer Analysis and Characterization, 23,181–192, 2017.

[14] M. M. EL-Zayat, R. M. Mohamed, H. A. Raslan. Evaluation of surface treatment and gamma irradiation on the performance of palm fiber/natural rubber biocomposites. Journal of Macromolecular Science, Part A. Pure and Applied Chemistry, 57, 344–354, 2019.

[15] E. Takács, L. Wojnárovits, J. Borsa, Cs. Földváry, P. Hargittai, O. Zöld. Effect of γ-irradiation on cotton-cellulose. Radiation Physics and Chemistry, 55, 663–666, 1999.

Biopolymer Applications Journal Lisa KLAAI et al. Vol 4, N°2, 2025, pp.10-15
e-ISSN : 2800-1729

Development of a Moisturizing Cream based on Prickly Pear Seed Oil

Lisa KLAAI[1,*], Dalila HAMMICHE[1]

[1]*Université de Bejaia, Faculté de Technologie, Laboratoire des Matériaux Polymères Avancés (LMPA), Route de Targa-Ouzemmour, Bejaia 06000, Algérie*

Corresponding author: lisa.klaai@univ-bejaia.dz*

Received: 10 April, 2025; Accepted: 24 May, 2025; Published: 4 July, 2025

Abstract

In this work, we developed a moisturizer based on prickly pear seed oil, highly valuable oil for its anti-aging benefits on the skin.
To achieve this, we conducted several research studies and analyses. First, we studied the raw materials: prickly pear seed oil, Shea butter, and surfactants, in order to create a stable oil-in-water emulsion. In the second part, we performed several tests and analyses: a centrifuge test, which allowed us to choose the right surfactants for a better emulsion; a pH test, which assesses the effectiveness of the cream produced. This is often considered a significant parameter in order to ensure a cream's pH is close to that of human skin; viscosity measurement determines whether it is viscous enough to be "sticky" or easy to spread; and finally, we performed five antibacterial tests: enumeration and detection of mesophilic aerobic bacteria, enumeration of yeasts and molds, Staphylococcus aureus, detection of Pseudomonas aeruginosa, and detection of Escherichia coli. From this, we obtained our glossy, white, highly viscous moisturizer with a pleasant odor that poses no harmful effects on human skin.
Keywords: *Prickly Pear Seed Oil, Moisturizer, Skin, Shea Butter, Emulsion.*

I. Introduction

The skin is defined as the outer covering of the mammalian body [1]. In humans, it occupies approximately 1.8 m² of surface area and represents 16% of the total body weight [2, 3]. It has three superimposed tissues in its structure: the epidermis, the dermis and the hypodermis. The dermis is the site of insertion of the skin appendages, represented by the appendages (hair and nails), the sebaceous glands and the sweat glands [4].

The skin has many functions mainly involved in maintaining the body's homeostasis, and in particular in thermoregulation and defense against external aggressions [5, 6]. It also plays a role in sensory and metabolic functions such as the synthesis of vitamin D [7].

For a long time, natural cosmetics remained unattractive, but today, against all expectations, they are experiencing a real boom among consumers. This means that the beauty industry is undergoing a complete revival, with the rise of natural products [8]. Therefore, we thought of formulating emulsions based on a natural product (prickly pear oil), Rich in vitamin E, omega-6 and sterols makes this precious oil an exceptional ingredient for fighting the signs of skin aging. It works wonders for maintaining the suppleness and tone of the skin [9]. Emulsions are thermodynamically unstable formulations. Knowledge of emulsion stabilization mechanisms and the development of new formulations are therefore of great importance; for this purpose, all tests were characterized microscopically, physico-chemically and rheologically. The formulation of these emulsions is based on the addition of the following excipients: water (aqueous phase), prickly pear seed oil (oily phase).

II. Material and methods

Prickly pear seed oil (PPSO) has been purchased from a Vegetable Oils Extraction, Micro-Enterprise, Algeria.

Shea butter was purchased from a store under the Commercial name "BEURRE ROYAL" in Bejaia, Algeria. This version of Shea Butter is a raw, unrefined, and undeodorized quality.

Vaseline oil was purchased from a store under the Commercial name "ELEIS" in Bejaia, Algeria.

Xanthan Gum in fine powder form, Loss on drying (%): 15. PH (1% solution): 6.0-8.0.

Glycerol (MW=92.09) was used to ensure optimal stability and reliability of the cream.

Polysorbitale 80 and Sorbitan monoaleate:

- Tween 80: is a non-ionic surfactant solution used as a supplement in various culture media in a laboratory setting. The name "Polysorbate 80" is a synonym for Tween 80, which has an HLB of 15.
- Span 80: Named polysorbate 80, it is a nonionic surfactant and emulsifier often used in foods and cosmetics. This synthetic compound is a viscous yellow liquid that is soluble in water.

Phenoxyethanol (MW=138.16), it is a synthetic preservative (prevents the development of microorganisms).

II.1. Preparation of the emulsion

We chose to formulate aqueous emulsions of the oil-in-water (O/W) type for their good tolerance, their strong penetrating power (unlike W/O emulsions which are weak), thanks to the auxiliary substances (wetting surfactants and emulsifiers) and since they are washable with water, which is not the case for W/O emulsions [10,11].

O/W emulsions undergo more transformations from the vehicle after application:

Friction causes the aqueous phase to evaporate, resulting in a cooling effect. Because these emulsions do not leave an oily film on the skin's surface, they can release lipophilic materials into the skin as well as water-soluble molecules from the continuous phase.

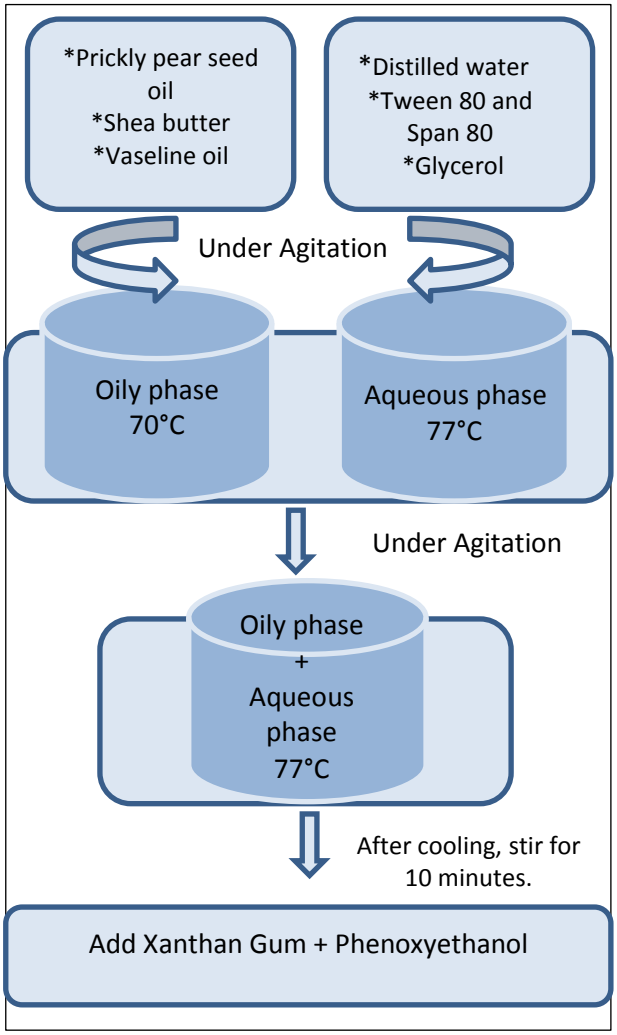

Figure1: Experimental protocol

II.1.1. Amount of Span 80 and Tween 80

The required amount of surfactants (Tween 80 and Span 80) in the formulation of each emulsion test was imposed by respecting the equation, giving the HLB of the mixture of two surfactants of different HLB [12].

$$HLB_{mixture} = [HLB_A * X_A + HLB_B (100-X_A)] / 100.$$

II.2. Formulation test

The aim of this section is to optimize the various proportions of compounds used in the formulation. To achieve this, we use the design of experiments method, which allows us to plan formulation tests, streamline the number of trials, and ensure the quality of the results.

We worked on six formulations (F1-F6).

II.3. Characterization of emulsions

II.3.1. Centrifuge Test

The stability of our formulation over time and under rigorous physical conditions was determined using a centrifuge (NEUATION iFuge C4000) set at 4000 rpm for 20 min.

II.3.2. Potentiometric measurement (pH measurement)

Once the device is calibrated, first wash the electrodes with distilled water. Homogenize the sample, add a sufficient volume to the measuring container, and immerse the electrodes. Check that the pH meter reading remains stable after one minute. Then record the pH. The pH meter used in this section is from AZ Instruments.

II.3.3. Viscometric analysis

The active part of the viscometer (VISCO ^{TM}) is a vibrating rod driven by a constant electrical supply. The amplitude of the vibration varies according to the viscosity of the fluid in which the rod is immersed. Its digital display allows a direct reading of the viscosity.

II.3.4. Bacteriological analysis

In our work, carried out five tests anti-bacterial enumeration and detection of aerobic mesophilic bacteria, enumeration of yeasts and molds, Staphylococcus aureus, detection of Pseudomonas aeruginosa, detection of Escherichia coli [13].

a. Preparation of culture media

Liquefy the Muller Hinton culture media for bacteria in a 95°C water bath and keep supercooled in a 45°C incubator.

- Under a laminar flow hood, aseptically pour the culture media into Petri dishes at a rate of 15 ml per dish.
- Allow to cool and solidify at room temperature, and store under conditions that prevent any alteration of their composition.

b. Seeding

- Aseptically soak a swab with the microbial suspension.
- Wring the swab by firmly pressing and twisting the inner wall of the tube to remove excess suspension.
- Aseptically inoculate a Petri dish by gently rubbing the swab across the surface of the Muller Hinton in tight lines.

c. Disk deposit

- Aseptically remove a sterile 6 mm diameter disc using sterile forceps.
- Place the tip of the disc in contact with the cream solution of known concentration, which will be absorbed by capillary action.
- Place the disc, thus soaked in cream solution, on the surface of the Muller Hinton, in the center of the Petri dish.
- Incubate the dishes at 37°C for 24 hours for bacteria.

- The medium is then inoculated with a determined level of microorganisms and, after incubation, the presence or absence of culture is noted; reading can be visual or spectrophotometric, as the degree of inhibition is related to the turbidity of the medium.

III. Results and discussion

III.1. pH measurement result

The results obtained show that the pH values of the different formulations are relatively variable, ranging between ($5.58 \leq pH \leq 6.17$) and are grouped in the following table:

Table 1: Results of pH measurement.

Formulation	F1	F2	F3	F4	F5	F6	F7
pH	5, 58	5,52	5,00	5,59	6,55	5,70	6,17

The most important elements of chemical stability are performance in accelerated tests and pH kinetics. When it comes to cream efficacy, pH is often considered a significant parameter.

The pH of human skin normally ranges from 4.5 to 7, and 5.5 is considered an average pH of human skin.

According to the measurement, the pH of formula (F4) is 5.59, close to the pH of the skin.

We can therefore say that this formulation is compatible with our skin and presents no risk of irritation [13].

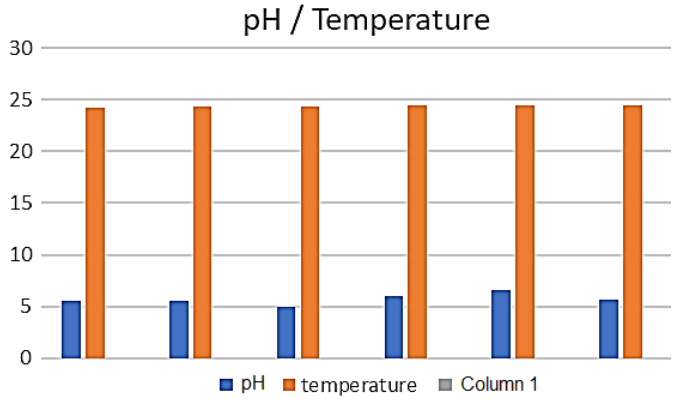

Figure 1: pH results a function of temperature.

III.2. Viscosity rate

Viscosity measurement allows us to know the flow properties of a formulation; the latter is sufficiently viscous, "sticky" or easy to spread [14]. The results of the measurement of the viscosity of the cream are shown in the following table:

Table 2: Viscosity rate measurement

Formulation	Viscosity (MPa.S)	Temperature (°C)
F 1	267	23,8
F 2	352	23,9
F 3	619	24,4
F 4	929	24,4

Viscosity differs for the four emulsion formulas prepared with the same HLB for use in cream form.

The results obtained show that the thicker the fluid, the higher the viscosity; however, the thinner the fluid, the lower the viscosity. In general, more viscous emulsions tend to have better stability over time. The results of our viscosity measurements show that the most viscous formulations generally correspond to those containing a high amount of xanthan gum, with varying percentages (15-40). Similar result reported in literature [15].

Because xanthan gum is a texturizing agent that allows the preparation to gel when cold, this indicates that it is a stabilizer and thickener, therefore increasing the viscosity of the emulsion [15].

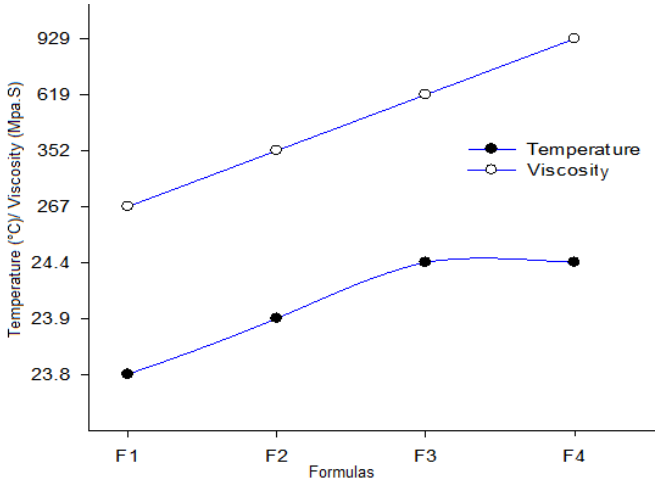

Figure 2: Evolution of the viscosity rate of different formulations

III.3. Centrifuge Test

The results revealed three distinct phases:

An organic phase in the supper part of the tube, and an aqueous phase in the lower part. These two phases are separated by a solid phase in the middle.

The results of the measurement of different stabilities of the cream are shown in the following table:

Table 3: Dilution results at different HLBs, (Phase separation (+); no phase separation (-))

Formulation	HLB	Dilution results
F1	8	-
F2	9	-
F3	10	-
F4	11	+
F5	12	+
F6	13	+
F7	14	-

✓ The chosen formula is the fourth formula

III.4. Antibacterial test

The antibacterial effect of the cream was tested by choosing five bacterial strains known for their resistance and the most used. After incubation at 32.5 °C ± 2.5 °C, for at least 24 hours (maximum 48 hours) absence of microbial growth. This means that our cream is of good microbiological quality.

IV. Conclusions

The objective of this work is to develop a moisturizer based on prickly pear seed oil, which is the active ingredient.

To achieve this goal and formulate a high-quality moisturizer, it is necessary to use virgin, cold-pressed oils.

We created an oil-in-water emulsion, respecting the standards for all the constituents of these two phases. This allowed us to obtain a moisturizer with a homogeneous, light texture, a

feeling of freshness and softness after use, with a sticky effect and good shine, and which spreads and penetrates the skin easily.

- According to the measurement, the pH of the developed cream is close to the pH of human skin.
- Viscosity measurement allows us to determine the flow properties of a formulation; it is sufficiently viscous, "sticky," or easy to spread.
- The developed cream poses no harmful effects or complications for the user.

The results of these analyses show that our cream is a light, moisturizing cream that spreads and penetrates the skin easily. It is very rich in antioxidants and vitamin E. The oils it contains are virgin and of high quality, and it meets all the criteria for commercialization.

References

[1] M.Y. Ferraq. Développement D'un Modèle De Cicatrisation Épidermique Après Une Désépidermisation Laser. Thèse d'Ingénierie Médicale et Biologique, U.F.R Médecine Paul Sabatier Toulouse, Université Toulouse III, p17, (2007)

[2] H. FERSADO. Etude de la libération de principes actifs depuis les émulsions concentrées: caractérisation et modélisation » Thèse de doctorat: Institut National Polytechnique de Lorraine, (2011)

[3] L. Gilbert. Caractérisation physico-chimique et sensorielle d'ingrédients cosmétiques : une approche méthodologique, Université du Havre, (2012)

[4] P.M. Elias. Stratum Corneum Defensive Functions: An Integrated View. Journal of Investigative Dermatology. 183–200, (2005)

[5] U. Heinrich, B. Garbe, H. Tronnier. In vivo Assessment of Ectoin: A Randomized, Vehicle-Controlled Clinical Trial. Skin PharmacolPhysiol. 20, 211–218, (2007)

[6] G. Peyrefitte, J. Camponovo. Esthétique-cosmétique. Tome 1 : biologie générale etcutanée – BTS esthétique-cosmétique. Paris, France: Elsevier-Masson. p.352, (2008)

[7] J.J. Towey, L. Dougan (2012) Structural examination of the impact of glycerol on water structure. Journal of Physical Chemistry B ,116,1633-1641, (2012)

[8] V. Isaac, L. Cefali, B. Chiari, C. Oliveira, H. Salgado, M. Correa. Protocolo para ensaios físicoquímicos d'estabilidade de fitocosméticos. Revista de Ciências Farmacêuticas básica e aplicada , 29, 81-96, (2008)

[9] P. Logeswari, S. Silambarasan, J. Abraham. Synthesis of silver nanoparticles using plants extract and analysis of their antimicrobial property. Journal of Saudi Chemical Society, 19, 311–317, (2015)

[10] T. Vemeil, A. Peter, C. Kelpatick. Hand hygiene in hospitals: anatomy of a revolution. Journal of Hospital Infection. 1, 320–327, (2018)

[11] M. Lodén. Role of topical emollients and moisturizers in the treatment of dry skin barrier disorders. American journal of clinical dermatology .4, 771-788, (2003)

[12] T. Lee, A. Friedman A. Skin barrier health: Regulation and repair of the stratum corneum and the role of over-the-counter skin care. Journal of Drugs in Dermatology 15,1047-1051, (2016)

[13] D. Bharathi, M. Diviya Josebin, S. Vasantharaj, V. Bhuvaneshwari. Biosynthesis of silver nanoparticles using stem bark extracts of Diospyros montana and their antioxidant and antibacterial activities. Journal of Nanostructure in Chemistry. 83–92, (2018)

[14] Z. Saddiqe, I. Naeem, A.J. Maimoona. A review of the antibacterial activity of Hypericum perforatum L. 131, 511-521, (2010)

[15] Y. Mouas, F.Z. Benrebiha, C. Chaouia. Evaluation de l'activité antibactérienne de l'huile essentielle et de l'extrait méthanolique du romarin rosmarinus officinalisL. RevueAgrobiologia,7, 363-370, (2017)

Biopolymer Applications Journal *Sofiane FATMI et al.* ***Vol 4, N°2, 2025, pp.16-19***
e-ISSN : 2800-1729

Development and validation of a routine UV spectroscopic method for determination of camptothecin in cyclodextrin complexes, liposomes, niosomes, and solid dispersions in PEG 6000

Sofiane FATMI [1,2,3*], Wassila BELKHIRI-BEDER [4], Hayet Ahlem LEZRAG [1,2,3], Zahra TOUTOU [1, 2], Lamia TAOUZINET [5], Malika LAHIANI-SKIBA [3], Mohamed SKIBA [3] and Mokrane IGUEROUADA [2]

[1] Université de Bejaia, Faculty of Technology, Department of Process Engineering, 06000 Bejaia, Algeria.

[2] Université de Bejaia, Faculty of Nature and Life Sciences, Associated Laboratory in Marine Ecosystems and Aquaculture, 06000 Bejaia, Algeria.

[3] Technology Pharmaceutical and Bio pharmaceutics Laboratory, UFR Medicine and Pharmacy, Rouen University, 22 Blvd. Gambetta, 76183, Rouen, France.

[4] Université de Bejaia, Faculté des Sciences de la Nature et de la Vie, Laboratoire de Biomathématique, Biophysique, Biochimie et Scientométrie, 06000, Bejaia, Algeria.

[5] Centre de Recherche en Technologies Agroalimentaires, Route de Targa Ouzemmour, Campus Universitaire, Bejaia 06000, Algeria.

*Corresponding author** sofiane.fatmi@univ-bejaia.dz

Received: 20 April, 2025; Accepted: 30 May, 2025; Published: 4 July, 2025

Abstract

A robust UV–Vis spectroscopic assay was developed and validated for quantifying camptothecin (CPT) in complex drug carriers, including cyclodextrin inclusion complexes, liposomal and niosomes suspensions, and PEG 6000 solid dispersions, addressing persistent analytical challenges posed by CPT's poor solubility and labile lactone ring. The method exhibited exceptional linearity over 1–50 µg·mL⁻¹ ($y = 0.0198 x + 0.0032$, $R^2 = 0.9991$), specificity with no interference from excipients (102.17 % recovery; RSD = 0.85 %), and accuracy/precision meeting ICH Q2 criteria (mean recovery = 99.96 %; RSD < 2 %). The limit of detection (0.5 µg·mL⁻¹) and quantification (1.5 µg·mL⁻¹) enabled rapid (< 5 min) throughput without the need for costly HPLC columns or organic solvents, substantially reducing per-sample cost and environmental burden. This UV method not only surpasses many chromatographic techniques in speed and simplicity but also preserves the CPT lactone form by minimising exposure to aqueous neutral pH, thereby providing a reliable analytical tool for routine industrial quality control of advanced CPT formulations.

Keywords: *Camptothecin, UV–Vis spectrophotometry, analytical method validation, cyclodextrin inclusion complexes, liposomes, niosomes, PEG 6000 solid dispersions, drug delivery systems.*

I. Introduction

Camptothecin (CPT) (figure 1), a pentacyclic alkaloid derived from Camptotheca acuminata, has been a cornerstone in oncology since its discovery in the 1960s due to its unique inhibition of topoisomerase I, a critical enzyme in DNA replication [1]. Despite its potent antitumor activity, CPT's clinical application has been hindered by poor aqueous solubility (<0.1 µg/mL), pH-dependent instability (hydrolysis of the lactone ring to the inactive carboxylate form), and severe toxicity (e.g., myelosuppression, hemorrhagic cystitis) [2, 3]. To overcome these limitations, advanced delivery systems such as cyclodextrin complexes, liposomes, and PEG-based solid dispersions have been formulated to enhance solubility, stability, and targeted delivery [4, 5, 6].

Analytical methods for CPT quantification in these systems are pivotal for formulation optimization and quality control. While high-performance liquid chromatography (HPLC) and liquid chromatography-mass spectrometry (LC-MS) are widely employed for their sensitivity, these techniques are time-consuming, costly, and require specialized training [7]. UV spectroscopy, though less sensitive, offers a rapid, economical alternative, provided it is validated for specificity in complex matrices. Previous studies have validated UV methods for CPT (R2=0.9987) [8], but a comprehensive method applicable to multiple delivery systems remains lacking.

This study aims to develop a single UV method for CPT quantification across diverse delivery platforms, validate the method per ICH Q2 (R1) guidelines, emphasizing specificity in the presence of excipients, and compare performance with existing chromatographic and spectroscopic techniques.

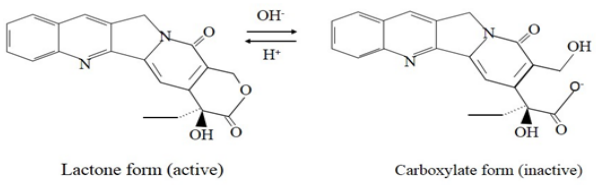

Figure 1: Camptothecin structure.

II. Material and methods

II.1. Chemicals and reagents

Camptothecin (CPT): Standard powder (≥98% purity, (M.w. 348.11 g/mol) was purchased from Shenzhen Boda Natural Product laboratory (P. R. China).
Cyclodextrins: α-CD, β-CD, γ-CD, HP β-CD, SBE β-CD and PM β-CD were obtained from Roquette Fréres (France).
Polyethylene glycol 6000 was obtained from BASF (Germany).
Phosphatidylcholine (Lipoid GmbH, SPC-3, purity >95%), cholesterol, and span 60 was obtained from (Merck).
Solvents: Ethanol (HPLC grade, Fisher Chemical), chloroform, methanol (analytical grade, Sigma-Aldrich).
Buffer solutions: Phosphate-buffered saline (PBS, pH 6.5–7.5) prepared using sodium dihydrogen phosphate and disodium hydrogen phosphate (Merck).

II.2. Formulation preparation

a) Cyclodextrin inclusion complexes

CPT and HP β-CD were combined in a 1:1 molar ratio and dissolved in 20 mL ethanol. The mixture was stirred (500 rpm, 24 h, 25°C) to ensure complexation, followed by solvent evaporation under reduced pressure (45°C, 200 mbar) using a rotary evaporator [9]. The dried complex was stored in amber vials at 4°C.

b) Liposomes and niosomes

Liposomes or niosomes: Phosphatidylcholine or Span 60 (non-ionic surfactant) (100 mg), cholesterol (20 mg), and CPT (5 mg) were dissolved in chloroform/methanol (2:1 v/v). The solvent was evaporated under vacuum (45°C, 100 mbar) to form a thin lipid film. The film was hydrated with PBS (pH 7.4, 10 mL) at 60°C for 1 h, followed by sonication (30 min, 40 kHz) to reduce vesicle size [10].

c) PEG 6000 solid dispersion

CPT (20 mg) and PEG 6000 (180 mg) were dissolved in 10 mL methanol under magnetic stirring (30 min). The solvent was evaporated at 45°C under reduced pressure. The resultant solid dispersion was pulverized, sieved (mesh size 100 µm), and stored in desiccators [4].

II.3. Method validation

Method validation was carried out in accordance with ICH Q2(R1) "Validation of Analytical Procedures: Text and Methodology" guidance to ensure the assay's fitness for purpose in quantifying camptothecin (CPT) within complex drug delivery matrices [11].
To assess specificity, blank formulations of each delivery system (cyclodextrin inclusion complexes, liposomal suspensions, niosomes and PEG 6000 solid dispersions) were prepared without CPT. UV–Vis spectra (300–400 nm) of these blanks were recorded and compared against samples spiked with 10 µg•mL^{-1} CPT or its equivalent to confirm the absence of interfering absorbance at the analytical wavelength (368 nm).
For linearity, a 1 mg•mL^{-1} CPT stock solution was prepared in ethanol and serially diluted to yield standards of 5, 10, 15, 25, 35 and 50 µg•mL^{-1}. Each concentration was measured in triplicate at 368 nm, and absorbance values were plotted versus nominal concentration to construct the calibration curve.
Accuracy was evaluated by spiking each blank delivery matrix at three concentration levels (10, 25 and 50 µg•mL^{-1}; n = 5 per level). Samples were processed and analysed by UV–Vis, with calculated concentrations compared to nominal values to determine percentage recovery.
Precision was determined at the mid concentration (25 µg•mL^{-1}) by replicate analysis (n = 3). Intraday precision was assessed by analysing all replicates on the same day, while inter day precision was evaluated over three consecutive days. Relative standard deviations (RSDs) were calculated for both repeatability and intermediate precision.
To verify robustness, the influence of minor procedural variations was examined by measuring CPT absorbance in phosphate-buffered saline adjusted to pH 6.5, 7.0 and 7.5, and at temperatures of 20 °C and 25 °C. RSDs of absorbance readings under these conditions were used to confirm the method's resilience to small changes in analytical parameters.

II.3. Characterization

UV-Vis spectrophotometer: Shimadzu UV-1800 (Kyoto, Japan), equipped with 1 cm quartz cuvettes. Instrument parameters: λ = 368 nm (CPT's absorption maximum, confirmed via full-wavelength scan).

III. Results and discussion

III.1. Specificity and matrix compatibility

No spectral interference was observed from cyclodextrins, lipid components, surfactant, or PEG 6000 excipients at the CPT λ_{max}, and blank-matrix scans confirmed the absence of co-absorbing species. Recovery of CPT from spiked vesicular matrices and encapsulated in cyclodextrin one was for the both 102.17% (RSD = 0.85%), well within the FDA's 90–110% acceptance criteria for bioanalytical recovery [11]. This high selectivity align with prior UV methods for CPT in microspheres (98.5% recovery) and matches also with LC-MS protocols reporting ~101% recovery in liposomal CPT [7, 8].

III.2. Linearity and sensitivity

Calibration over 1–50 µg/mL displayed excellent linearity ($y = 0.0198x + 0.0032$, $R^2 = 0.9991$) (Figure 1), consistent with reported UV studies on CPT ($R^2 = 0.998$) [8]. The limit of detection (LOD) and quantification (LOQ) were determined as 0.5 µg/mL and 1.5 µg/mL, respectively, using signal to noise criteria (3:1 and 10:1). While sufficient for formulation assays, these thresholds are higher than ng/mL sensitivities of LC MS methods (LOD ~10 ng/mL) and may limit pharmacokinetic application [12].

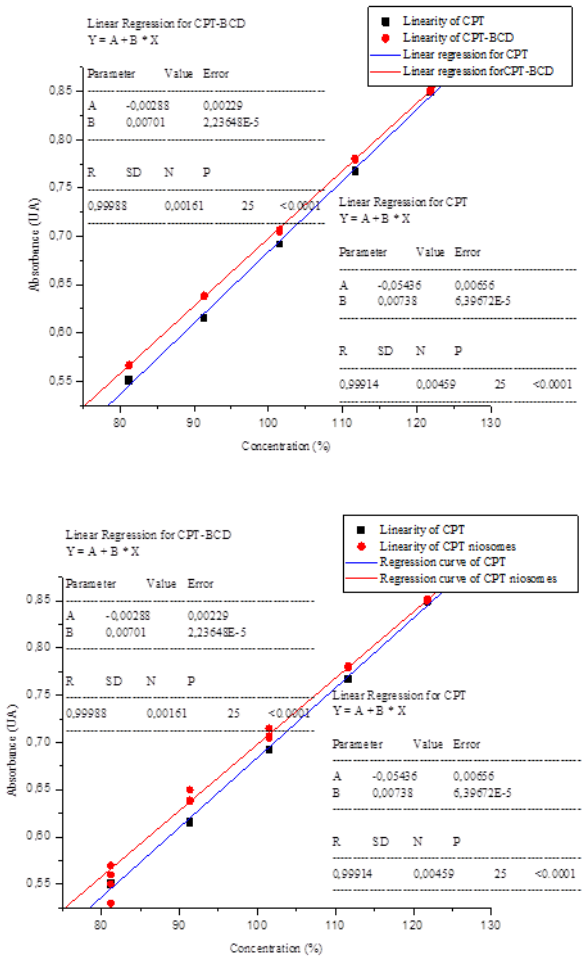

Figure 2: Linearity of captothecin, camptothecin- HP β-CD and liposomes of camptothecin.

III.3. Precision and accuracy

Across low, mid, and high QC levels, mean recovery was 99.96% (overall RSD < 1.5%), with intra and inter day RSD values consistently < 2% (Table 1). These precision metrics outperform reported LC MS assays for liposomal CPT [13, 14] and comply with ICH Q2 (R1) guidelines [11].

Table 1: Precision and recovery data for camptothecin liposome and encapsulated in HP β-CD.

Sample	Added standard (µg/mL)	Linearity (R2)	Accuracy (%recovery)	Precision (%RSD)		L.D (µg/ml)	L.Q (µg/ml)
				Intra-day	Inter-day		
CPT/ HP β-CD	25	0.998	99.88	0,29	0,19	0.5	1.5
	25		99.6				
	25		99.6				
	25		99.74				
	25		99.705				
CPT liposome	25	0.998	99.6	0,3	0,2	0.5	1.5
	25		100.31				
s	25		99.88				
	25		99.88				
	25		99.92				

III.4. Robustness under variable conditions

Deliberate modifications of buffer pH (6.5–7.5) and ambient temperature (20–25 °C) produced absorbance RSD < 1.8%, confirming analytical robustness. Such resilience is critical given CPT's known sensitivity to pH and temperature, where the lactone ring can hydrolyze.

III.5. Comparative advantages

Compared to HPLC, which typically requires 20–30 min per run and costly HPLC grade acetonitrile , the UV assay completes analysis in < 5 min without high pressure instrumentation or extensive sample preparation. The cost effectiveness is particularly advantageous for routine formulation quality control (QC), where throughput and reagent costs are key constraints [15].

III.6. Addressing CPT Instability

CPT's lactone to carboxylate conversion at neutral pH can lead to underestimation in slower methods. The rapid UV analysis minimizes exposure time, preserving the active form and yielding more accurate concentrations than LC MS methods with longer run times (~ 10 min) that may underestimate lactone content [16, 17].

III.7. Limitations and future directions

While the LOD of 0.5 µg/mL meets formulation needs, enhancement to ng/mL sensitivity is desirable for pharmacokinetic or biodistribution studies. Integration of pre concentration steps—such as solid phase extraction (SPE) or dispersive micro solid phase extraction—could lower detection limits without sacrificing speed [13, 14].

IV. Conclusions

This study presents a validated UV–Vis spectrophotometric protocol that fulfils both FDA bioanalytical validation guidance (102.17 % recovery within 90–110 %) and ICH Q2(R1) performance standards (precision and accuracy RSD < 2 %), offering a pragmatic alternative to more resource intensive HPLC or LC MS methods. The assay's linear dynamic range (1–50 µg•mL^{-1}, R^2 = 0.9991) and LOD of 0.5 µg•mL^{-1} ensure robust quantification of CPT across diverse delivery matrices without spectral interference from cyclodextrins, phospholipids, surfactants or polyethylene glycol. Critically, its sub five minute run time and elimination of expensive chromatographic consumables markedly enhance laboratory throughput and reduce operational costs. By preserving the delicate CPT lactone form, the method mitigates underestimation of active drug levels that can afflict slower chromatographic analyses.

The described UV–Vis method provides a fast, accurate and cost effective analytical foundation for industrial quality control of advanced CPT delivery systems, and sets the stage for future enhancements that bridge laboratory routine assays with high sensitivity bioanalysis.

.***References***

[1] C.J. Thomas, N.J. Rahier, S.M. Hecht. Camptothecin: Current Perspectives. Bioorganic & Medicinal Chemistry 12(7), 1585–1604, (2004). doi:10.1016/j.bmc.2003.11.036.

[2] M. Kamle, S. Pandhi, S. Mishra, et al. Camptothecin and Its Derivatives: Advancements, Mechanisms and Clinical Potential in Cancer Therapy. Medical Oncology 41(263), (2024). doi:10.1007/s12032-024-02527-x.

[3] S. Fatmi, L. Taouzinet, M. Lahiani-Skiba, et al. New Formulation and Evaluation of Camptothecin Encapsulated and/or Dispersed Suppository. Anti-Cancer Agents in Medicinal Chemistry 21(9), 1183–1190, (2021). doi:10.2174/1871520620666200903150635.

[4] S. Fatmi, L. Bournine, M. Iguer-Ouada, et al. Amorphous Solid Dispersion Studies of Camptothecin-Cyclodextrin Inclusion Complexes in PEG 6000. Acta Poloniae Pharmaceutica 72(1), 179–192, (2015). PMID:25850214.

[5] S. Fatmi, L. Taouzinet, M. Skiba, et al. Camptothecin: Solubility, In-Vitro Drug Release, and Effect on Human Red Blood Cells and Sperm Cold Preservation. CryoLetters 44(2), 89–99, (2023). doi:10.54680/fr23210110712.

[6] G.E. Flaten, T.T. Chang, W.T. Phillips, et al. Liposomal Formulations of Poorly Soluble Camptothecin: Drug Retention and Biodistribution. Journal of Liposome Research 23(1), 70–81, (2013). doi:10.3109/08982104.2012.742537.

[7] Q. Li, Q. Zhu, X. Zhang, et al. A Liquid Chromatography–Tandem Mass Spectrometry Method for Pharmacokinetics and Tissue Distribution of a Camptothecin Quaternary Derivative in Rats. Fitoterapia 90, 57–64, (2013). doi:10.1016/j.fitote.2013.06.012.

[8] S.T. Galatage, R. Trivedi, D.A. Bhagwat. Characterization of Camptothecin by Analytical Methods and Determination of Anticancer Potential Against Prostate Cancer. Future Journal of Pharmaceutical Sciences 7(104), (2021). doi:10.1186/s43094-021-00236-0.

[9] S. Fatmi, L. Taouzinet, Z. Toutou, et al. Stability Ring Lactone Study of Camptothecin and Irinotecan in Artificial Media and Human Plasma. Biopolymer Applications Journal 1(1), 1–5, (2022). ISSN:2800-1729.

[10] A.M. Sætern, M. Skar, Å. Braaten, et al. Camptothecin-Catalyzed Phospholipid Hydrolysis in Liposomes. International Journal of Pharmaceutics 288(1), 73–80, (2005). doi:10.1016/j.ijpharm.2004.09.010.

[11] J. Ermer. ICH Q2 (R2): Validation of Analytical Procedures. Method Validation in Pharmaceutical Analysis: A Guide to Best Practice, 351–372, (2025). doi:10.1002/9783527831708.ch13.

[12] Z. Wang, C. Shao, Z. Hu, et al. The Development and Validation of an LC-MS/MS Method for the Quantification of CZ112, a Prodrug of 9-Nitrocamptothecin in Rat Plasma. Journal of Pharmaceutical and Biomedical Analysis 179, 112963, (2020). doi:10.1016/j.jpba.2019.112963.

[13] S. Khan, A. Ahmad, W. Guo, et al. A Simple and Sensitive LC/MS/MS Assay for 7-Ethyl-10-Hydroxycamptothecin (SN-38) in Mouse Plasma and Tissues: Application to Pharmacokinetic Study of Liposome Entrapped SN-38 (LE-SN38). Journal of Pharmaceutical and Biomedical Analysis 37(1), 135–142, (2005). doi:10.1016/j.jpba.2004.09.053.

[14] E. Ghazaly, J. Perry, C. Kitromilidou, et al. Development and Validation of an Ultra-High Performance LC-MS/MS Assay for Intracellular SN-38 in Human Solid Tumour Cell Lines: Comparison with a Validated HPLC-Fluorescence Method. Journal of Chromatography B 969, 213–218, (2014). doi:10.1016/j.jchromb.2014.08.024.

[15] Q. Wang, G. Wang, S. Xie, et al. Comparison of High-Performance Liquid Chromatography and Ultraviolet-Visible Spectrophotometry to Determine the Best Method to Assess Levofloxacin Released from Mesoporous Silica Microspheres/Nano-Hydroxyapatite Composite Scaffolds. Experimental and Therapeutic Medicine 17(4), 2694–2702, (2019). doi:10.3892/etm.2019.7238.

[16] L.P. Rivory, E. Chatelut, P. Canal, et al. Kinetics of the in Vivo Interconversion of the Carboxylate and Lactone Forms of Irinotecan (CPT-11) and of Its Metabolite SN-38 in Patients. Cancer Research 54(24), 6330–6333, (1994).

[17] J. Fassberg, V.J. Stella. A Kinetic and Mechanistic Study of the Hydrolysis of Camptothecin and Some Analogues. Journal of Pharmaceutical Sciences 81(7), 676–684, (1992). doi:10.1002/jps.2600810718.

Biopolymer Applications Journal Chadia IHAMOUCHEN. Vol 4, N°2, 2025, pp.20-26
e-ISSN : 2800-1729

Effect of olive husk flour silanization on the mechanical and thermal properties of high-density polyethylene composites

Chadia IHAMOUCHEN [1*]
[1] *Laboratoire des Matériaux Polymères, Faculté de Technologie Avancés, Université de Bejaia Route de Targa Ouzemour, Bejaia 06000, Algérie*
Corresponding author: Chadia.benmerad@univ-bejaia.dz*
Received: 01 May, 2025; Accepted: 25 June, 2025; Published: 4 July, 2025

Abstract

The present paper summarizes an experimental study on the mechanical and thermal behavior of olive husk flour (OHF) reinforced high-density polyethylene (HDPE) composites. Several formulations of PE filled with 10, 20 and 30 % by weight of untreated olive husk and that treated with vinyltriacetoxy-silane (VTAS) were prepared. Fourier transform infrared (FTIR) spectroscopy was used to analyse involved silanization reactions. Scanning electron microscopy (SEM) was used to show the morphology of the flour surface. Furthermore, the mechanical and thermal characteristics of the various composite samples were investigated as a function of both loading contents and chemical treatment. The results showed that the properties of the composite materials are positively affected by silanization treatment of OHF.
Keywords: *composites, high-density poly(ethylene) (HDPE), olive husk flour, surface treatments, silanization.*

I. Introduction

Interest in the development of new composite materials derived from natural fibers and thermoplastic polymer matrices has grown markedly in the last years because there are environmental and economic advantages to produce wood flour thermoplastic composites. These composites are being used in a large number of applications, including automotive, interiors, building industry and many other furnitures [1,2].
Wood fillers can be combined with both thermosets and thermoplastics such as high density polyethylene (HDPE), which is one of the most important thermoplastics due to its good properties, i.e. fluidity, flexibility, electrical insulation, etc [3].
Olive husk is an agricultural residue produced as industrial by-products of olive milling. Every year, thousands of tons of this product are incinerated or rejected in the wild by causing major inconvenience to the environment, despite the fact that this product has significant advantages as a wood filler compared to mineral fillers, such as lightness, high stiffness, low cost, and renewable materials. However, their association with plastics, in particular polyolefins however, presents a major inconvenience. They have a strong affinity with water which creates incompatibility at interfaces between wood particles and hydrophobic thermoplastic causing swelling inside the material and subsequently, a deterioration of all mechanical properties [4,5] To solve the problem of incompatibility, it appears necessary to develop solutions through the use of chemical treatments. The chemical treatment of wood filler or the functionalization of the polymer usually requires the use of reagents, which contain functional groups that are capable of reacting and form chemical bonds with the hydroxyl groups of the lignocellulosic material [6-8]. A lot of research was devoted to composites based on HDPE and lignocellulosic fillers, but only few works ware published on polymer composites loaded with olive husk flour. In this work, composites based on HDPE and olive husk flour before and after treatment with vinyltriacetoxy-silane was studied. Moreover, the effects of the treatment on the mechanical, morphological and thermal properties of the composites were also investigated.

II. Experimental

a. Materials

High-density polyethylene used is "POLYMED 6030", (MFI= 2-3 g/10 min, 190°C/2.16Kg). Sigma Aldrich Company (Germany) produced the vinyltriacetoxy-silane (VTAS). The main characteristics of the product are: density = 1.167g/cm^3, melting point = 76°C and boiling point = 126 – 128°C. Olive husk flour (< 100 μm) from Béjaïa, Algeria

b. Flour treatment

10 g of olive husk flour were added into a mixture of methanol/water (90/10, w/w) and stirred for 12 h at room temperature. The flour was then filtered and dried in an oven at 80 °C for 12 h. For the flour surface treatment, 5% (wt/wt) of vinyl triacetoxy silane was dissolved in a methanol/water mixture at room temperature and the pH of the solution adjusted to 4 with the addition of acetic acid. After the continuous stirring of the solution for 10 min, the dried olive husk flour was immersed in the solution and stirred for 24 h at room temperature. The olive husk flour was then filtered and dried at 80°C for 12h [9].

Various formulations based on high-density polyethylene (HDPE), olive husk flour before (UTOHF) and after treatment with vinyl-triacetoxy-silane (OHFTS), were prepared, whose codes (UT: untreated, TS: treated with silane) and compositions are reported in table 1.

c. Preparation of Composites

Films were prepared by twin-roll milling process, using a rotating speed of 28.5 rpm for the back cylinder and 29.8 rpm for the front cylinder at 160°C and a residence time of 8 min. The gap in between the rolls is roughly 1 mm. The films were then granulated and pressed into plates of 2 mm thick by using a hydraulic press model FONTUME HOLAND at 180°C and 50 KN during 5 min. The plates obtained were used for testing.

d. Spectroscopic analysis (FTIR)

The reaction product was qualitatively characterized by FTIR, using KBr pellet technique. Spectra were recorded using an infrared spectrophotometer Fourier transform (FTIR) model *SHIMADZU FTIR-8400* with a resolution of 4 cm^{-1} within the region 4000 - 400 $cm^{-1.}$

e. Tensile test

The tensile test is carried out using a tensile machine of the type *BTC-FR 2,5 TN.D09*, according to the standard ISO 527, June 1993. The speed of deformation is maintained constant at 50 mm/min. The curves strength-deformation are plotted, each value obtained represents the average of six samples.

f. Thermogravimetric analysis

Thermogravimetric analysis aims to assess the loss of mass that undergoes a sample during a heat treatment as a function of temperature. The apparatus used is type *SETARAM TGA 92* ", consisting of a TGA / DTG / ATD coupled and driven by a microcomputer. The experiments were conducted on samples of mass from 10 to 20 mg, which are built in a crucible and heated in platin in an inert nitrogen with a heating rate of about 10 °C/min and in a temperature range from 20 to 700 ° C.

g. Test of water absorption

Composite samples were used for measuring water absorption according to the following procedure: after being oven-dried at 70°C for 24 h, the specimens were kept in the desiccators at room temperature. Then, the specimens were weighted before immersion in distilled water and the corresponding mass was recorded as (M_0). The specimens were periodically removed from the water bath, surface dried with absorbent paper, and weighed again. The corresponding mass was defined as (M). Three specimens were tested for each compound and the average readings were recorded. Water absorption was calculated according to standard NF 51-002.

h. Scanning electron microscopy

Scanning electron microscopy (SEM) was performed with a ***FEI CONTA 200*** microscope. Before the fracture, the specimens were frozen into liquid nitrogen to impede the plastic deformation of the matrix and to get well defined fiber–matrix interface. The objective was to get some information regarding the filler dispersion and bonding quality between filler and matrix and to detect the presence of microdefects.

Table I. Mass composition of the various PE formulations

Components	F0	F10 UT	F20 UT	F30 UT	F10 TS	F20 TS	F30 TS
HDPE [% wt]	100	90	80	70	90	80	70
UTOHF [% wt]	0	10	20	30	0	0	0
OUFTS [% wt]	0	0	0	0	10	20	30

III. Results and discussion

a. Fourier transform infrared spectroscopy

FTIR spectra of both untreated and silanized olive husk flour are presented in figure 1. In the silanized olive husk flour, it is clearly observed the appearance of the same peaks as for untreated OHF. The only difference noted is related to the absorption band located in the range 3700 and 3050 cm^{-1}, which corresponds to the elongation vibrations of hydroxyl groups (-OH), for which there is a decrease in intensity compared to the untreated olive husk flour (UTOHF). This decrease as reported by Kaci and Bengtsson [10,11] was attributed mainly to the diminution of the hydrophilic character of the olive husk flour after treatment.

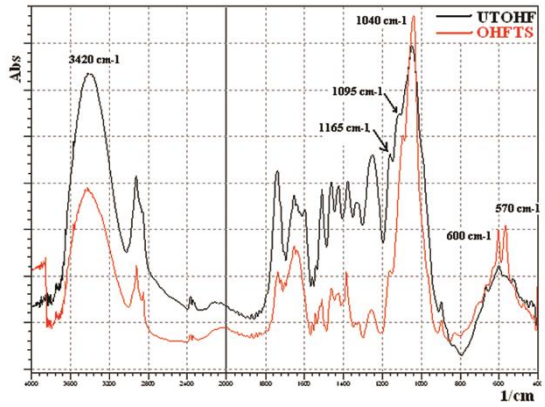

Figure 1: Spectra (FTIR) of the olive husk flour untreated and treated

It was also noticed an absorption band at 1165 cm^{-1} which can be assigned to Si-O-
cell or Si-O-Si groups, the first confirms the grafting of silane on fibers and the second is an indication that the intermolecular condensation is produced between adjacent silanols groups. There are also one absorption band centred at 1095 cm^{-1}, characteristic of Si-O-Si vibration; this could be attributed to the substitution of OH groups from olive husk flour by silanol groups (obtained during hydrolysis of silanes) by condensation reaction, indicating the occurrence of silanisation reaction [12]. The peak near 1039 cm^{-1} of the treated flour is related to the residual unhydrolyzed Si–O–CH_3 groups; the weak intensity suggests that most of the silane was hydrolyzed. We also observe an absorption band in the region of 1625 cm^{-1} attributed to connection (C=C) of the vinyl groups of the coupling agent. FTIR analysis confirms that the reaction of silanisation took place, which makes it possible is to propose a suitable reactional mechanism for this modification (See Scheme 1) [13].

b. Mechanical properties

The evolution of the elongation at break and Young's modulus of untreated and treated PE composites as a function of wood filler loadings is presented in figure 2 and 3, respectively. It is observed that the deformation of the untreated HDPE/ OHF composites decrease linearly with increasing the flour loading up to 30%. These results are expected and are in agreement with literature. Kaci and Kim [10, 14] have attributed this decline to the decrease of the strength of connection between the filler and the matrix that blocks the spread of effort. This decline increases as the flour loading becomes higher; this can be explained by the tendency of particles of olive husk flour to form agglomerates which induce heterogeneities within the matrix. The addition of untreated OHF in the polyethylene matrix increases the Young's modulus of the composite and this becomes stronger with increasing the flour content. This behaviour can be explained by the rigid nature of OHF.

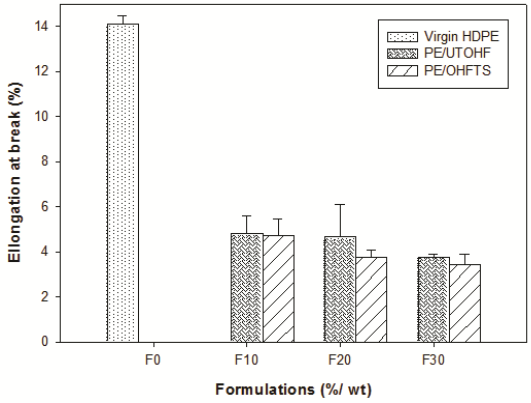

Figure 2: Evolution of elongation at break of composites PE/OHF

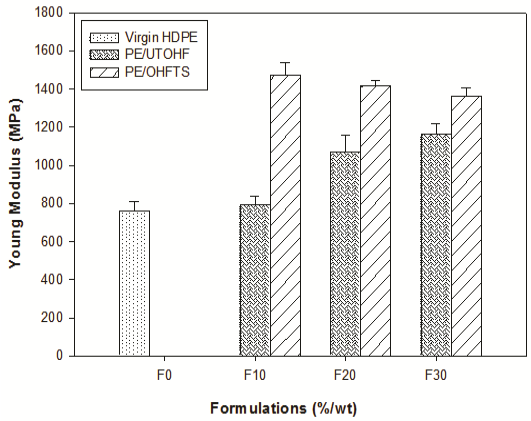

Figure 3: Evolution of Young modulus of composites PE/OHF

After chemical treatment, the elongation at break decrease compared to the untreated composites, but not in terms of overall deformation compared to virgin PE. This decrease is attributed to the good dispersion of the flour by adding the modifying agent which gives stiffness to the material [15, 16] Furthermore, we notice that the addition of treated flour with vinyl-silane induces a drastic increase in the Young's modulus. This increase is mainly due to greater interfacial adhesion matrix/filler due to the good dispersion of the treated filler in the PE matrix [17].

c. Thermal characterizations of composites

Figures 4, 5 and 6 show the TG and DTG thermograms of different composites prepared with untreated and treated loadings at 10, 20 and 30%, respectively. We notice that the addition of untreated olive husk flour in the PE matrix decreases the onset decomposition temperature and this decrease becomes higher with the flour content. This decrease can be attributed to the presence of three main components (cellulose, hemicellulose and lignin) in OHF as confirmed by Ersan Putun [18]. The cellulosic filler is degraded between 200 and 350°C, whereas PE is degraded at higher temperatures (400°C). Therefore, the thermal behaviour of the composite is the sum of the individual constituents of both filler and matrix. Around 460°C, there is a level of stability, attributed to the formation of a residue.

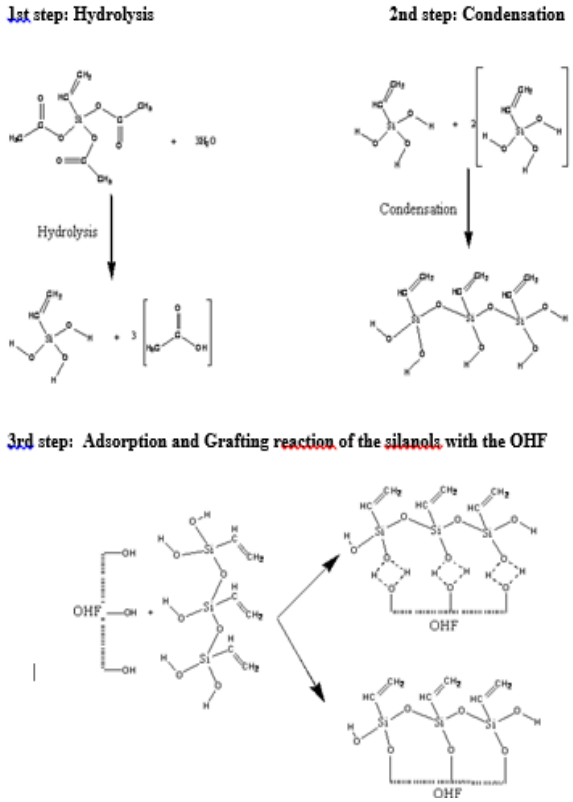

Scheme 1: Mechanism between the olive husk flour and the vinyltriacetoxysilane

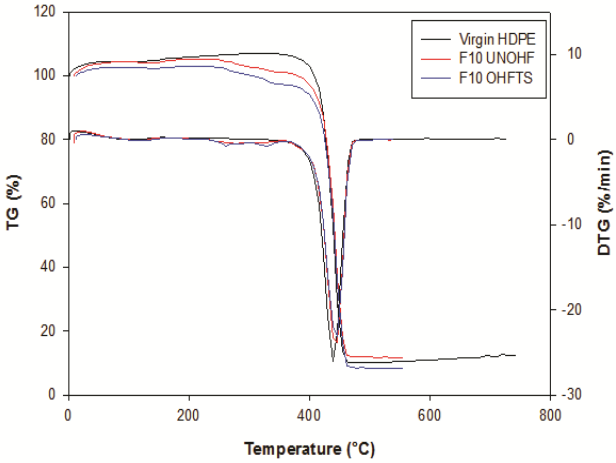

Figure 4: TG and DTG thermograms of different composites prepared with untreated and treated loadings at 20%.

For the DTG thermograms of untreated and treated composites, we see the formation of different endothermic peaks. A first peak appearing around 100°C, corresponds to the evaporation of water physically adsorbed on the surface of particles of untreated olive flour composites. The peaks areas is more important when the rate of untreated flour is

higher, this phenomenon can be attributed to the hydrophilic nature of untreated flour, which has the capacity to absorb more water. However, at the same temperature interval, polyethylene does not show any peak due to its hydrophobic character. A second peak corresponds to the thermal degradation of hemicellulose and cellulose and it is located between 200 and 300°C. More specifically, the thermal decomposition of cellulose occurs mainly by depolymerisation from 300°C [19, 20] Hemicellulose is less thermally stable than cellulose, and degrades between 200 and 260°C. In a study of jute fiber and its components by Bhaduri [21], they attributed this process to pyrolysis of the hemicellulose fraction. At approximately 350 ° C, a third peak appears, it corresponds to the decomposition of lignin. This process can be explained by the cleavage of carbon-carbon bond between the structural units of lignin and dehydration reactions between 380-470°C [14], a broader peak with high intensity appears and it corresponds to the polyethylene matrix decomposition. Beyond 500°C, there is stability due to the formation of residue. The effect of treatment in F10 formulation improves the thermal stability of the composite materials. On the contrary, to the treated formulations based on F20 and F30, the results show an increase in the onset decomposition temperature compared to untreated composites.

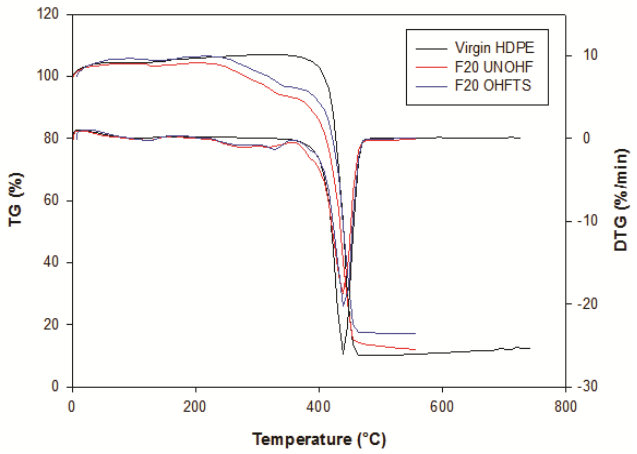

Figure 5: TG and DTG thermograms of different composites prepared with untreated and treated loadings at 10%.

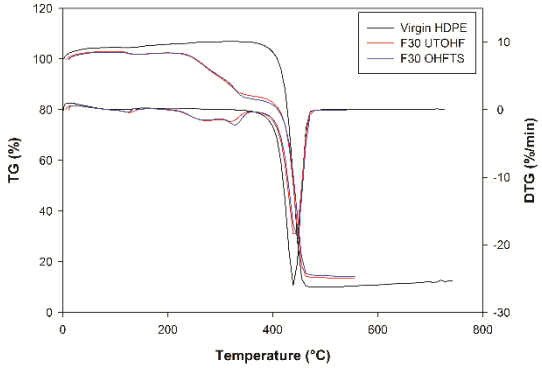

Figure 6: TG and DTG thermograms of different composites prepared with untreated and treated loadings at 30%.

d. Water absorption test

The evolution of water absorption of the composites HDPE/OHF as a function of time is shown in figure 7. We can clearly see an increase in the absorption rate of water with immersion time for the untreated olive husk flour, which is quite expected. Boufi and Dufresne [12, 22] reported the same result and they explained that the olive husk flour is highly rich in hydroxyl groups; they form hydrogen bonds with water molecules. For the virgin PE, there is very low water absorption due to apolar nature of this polymer, and its hydrophobic character. After silane-treatment of OHF, the rate of water absorption decreases. This result can be attributed to a diminution of the concentration of -OH groups of the cellulosic filler. However, the hydrophilic character is more pronounced for the untreated composites compared to the composites treated with modifying agent (vinyltriacetoxy-silane) [10,12].

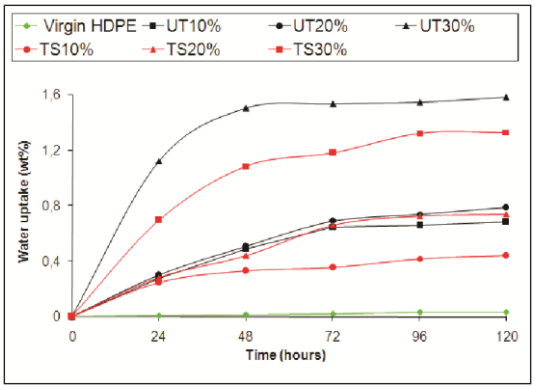

Figure 7: Evolution of the rate of water absorption of HDPE/OHF composites untreated and treated with silane.

e. Scanning electron microscopy

SEM micrographs of the fractured surface of HDPE-based composite reinforced with 20 wt% are shown in figure 8. For the untreated composites (figure.8a), we can see the presence of many voids and cavities on the surface, indicating that the

particles of olive husk flour are pulled out from the matrix during fracture. This observation indicates clearly that the interfacial adhesion between the cellulosic filler and the polymer matrix is very weak. The presence of olive husk aggregates provides an evidence of the poor dispersion of the filler within the polymeric matrix [23].

On the other hand, the SEM micrographs of the modified fillers with silane (figure. 8 b) seem to provide better and finer dispersion of the cellulosic fillers in HDPE and subsequently a strong interfacial adhesion has occurred between the olive husk filler and the polymer matrix. This behavior is due to the surface chemical modification, which confers a non-polar character to the surface of the cellulosic fillers [24]. However, the addition of olive hush flour treated with silane seems to enhance better the direct contact between the lignocellulosic fillers and the polymer matrix than the untreated composites.

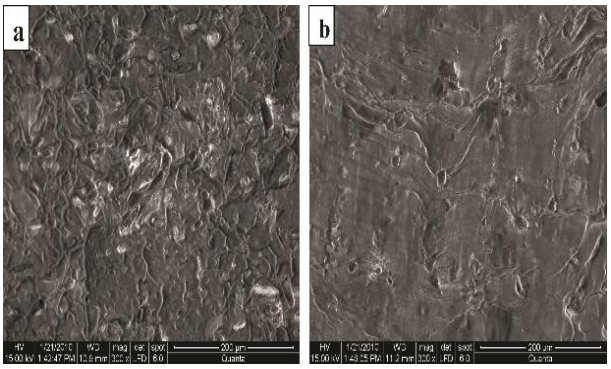

Figure 8: Scanning electron micrographs of fractured surface of HDPE /OHF composite loading at the 20 wt% (*700): (a) composite untreated (b) composite treated with silane

IV. Conclusion

The results of FTIR analysis of the OHF modified with vinyltriacetoxy-silane confirm the reaction of silanization. The results showed that the mechanical properties of the composite materials are positively affected by silanization treatment of OHF, when the untreated olive husk flour increases, the elongation at break decreases, while the Young modulus progressively increases. After chemical modification with the vinyl silane, the elongation at break also decreases and the Young's modulus increases for both composites but more pronounced for the modified ones. The thermal analysis has shown that the incorporation of the untreated olive husk flour in the PE matrix decreases the onset decomposition temperature. The effect of treatment for formulations F10 does a little improvement in thermal stability of composites. However, there is a gain in the temperature of the beginning of decomposition for formulations F20 and F30 compared to the untreated formulation. The rate of water absorption depends on the immersion time and the rate of olive husk flour, which gives a character more or less hydrophobic to the materials. These results are confirmed by scanning electron microscopy (SEM) micrographs.

References

[1] S.D .Roy, A. Massey, A. Adnot, A. Rjeb, Express Polymer Letters, 1(8), 506–511, (2007).

[2] K. Hyun-Joong, Y. Han-Seung, P. Michael, K. Hee-Soo, K. Sumin, Composite Structures, 79, 369–375 ,(2007).

[3] C. Panayiotou, V. Tserki, N.E. Zafeiropoulos, F. Simon, Composites: Part A, 36**,** 1110–1118 ,(2005).

[4] F. Corrales, F. Vilasec, M. Llop, J. Gironès, J.A. M´endez, P. Mutj, Journal of Hazardous Materials, 144, 730–735 ,(2007).

[5] A. K.Bledzki, F.Omar, Composites Science and Technology , 64, 693–700 ,(2004).

[6] S. Marais, A. Bessadok, F. Gouanve, L. Colasse, I. Zimmerlin, S. Roudesli, M.Métayer, Composites Science and Technology, 67, 685–697 ,(2007).

[7] A. Viksne, A.K. Bledzki, M. Letman, L. Rence, Composites: Part A, 36, 789–797 ,(2005).

[8] J. Aurrekoetxea, M. Sarrionandia, X.G´omez, Wear, 265 (5-6), 606-611, (2008).

[9] J. Gassan, A.K. Bledzki, Composites: Part A, 28**,** 1001, (1997).

[10] M. Kaci, H. Djidjelli, A. Boukerrou, L. Zaidi, Express Polymer Letters, 1 (7), 467–473 (2007).

[11] M. Bengtsson, K. Oksman, Composites: Part A, 37, 752–765, (2006).

[12] S. Boufi, M. Abdelmouleh, M.N. Belgacem, A. Dufresne, Composites Science and Technology , 67, 1627–1639, (2007).

[13] A. Boukerrou, S. Krim, H. Djidjelli, C. Ihamouchen, J.Martinez, Journal of Applied Polymer Science, 122, 1382–1394, (2011).

[14] K. Hyun-Joong, Y. Han-Seung, P.M. Wolcott, K. Hee-Soo, K. Sumin, Composite Structures, 79, 369–375, (2007).

[15] C. Nah, C.K. Hong, I. Hwang, N. Kim, D.H. Park, B.S. Hwang, Journal of Industrial and Engineering Chemistry, 14, 71–76, (2008).

[16] T. Sabu, J.M. Jacob, F. Bejoy, K.T. Varughese, Composites: Part A ,39 (2), 352-363, (2008).

[17] C. Ihamouchen, H. Djidjelli, A.Boukerrou, S. Krim, M. Kaci, J. Martinez, Journal of Applied Polymer Science, ***123,*** 1310–1319, (2011).

[18] P. Ersan, U.B. Burcu, A.E. Put. *J. Anal. Appl. Pyrolysis*, **79,** 147–153, (2007).

[19] D H.jidjelli, B.D.achour, A. Boukerrou, O. Zefouni, J. Martinez-Véga, J. Farenc, M .Kaci. Express Polymer Letters, **1,** 846–852, (2007).

[20]. K.J. Heritage, J. Mann, R. gonzales, Journal of Polymer Science: Part A **1,** 671-685, (1963).